# Research on Seismic Design and Stability Analysis of External Structures in Caves

Hairui Gou[1,a], Guanzhong Wu[1,2,3,*], Qingzhao Ren[1,b], Shaochi Peng[2,3,c], Wensong Wang[2,3,d]

[1]China Railway Cultural Heritage rehabilitation Technology Innovation Co., Ltd., Chengdu, China
[2]State Key Laboratory of Geohazard Prevention and Geoenvironment Protection, Chengdu University of Technology, Chengdu, China
[3]School of Environment and Civil Engineering, Chengdu University of Technology, Chengdu, China

[a]695367648@qq.com, [*]15055405095@163.com, [b]970499860@qq.com, [c]2411759220@qq.com, [d]wws@cdut.edu.cn

**Abstract.** Seismic forces significantly compromise the stability of subterranean caverns. This study focuses on the seismic support design process by using the Jiazhaerjia Cave as a case study. Initially, Prandtl's theory was employed to compute the design loads. Subsequently, optimal support mechanisms were identified through finite element simulations. The integration of the structural system with the surrounding rock mass was then analyzed to assess the stability of the structure under both seismic loads and natural conditions. The findings indicate that the proposed support structure exhibits robust seismic resistance, fulfilling the seismic mitigation requirements of the cavern. This study contributes to the framework for analyzing support schemes for similar cavern configurations.

**Keywords:** Seismic Loads; Seismic Structures; Structural Stability

## 1 Introduction

Cave murals are treasures of world culture, embodying the heritage of civilization and the memory of history [1]. However, the stability of caves under seismic loads is continually compromised, posing severe challenges to the preservation of these murals within. Consequently, research into the seismic design and stability analysis of external structures in caves holds significant engineering value.

Compared to static loads, the original rock is more prone to buckling under seismic loads [2-6]. Considerable progress has been made in the study of rock cave failures under seismic conditions. In terms of theoretical models, Wang et al. [7] proposed a dynamic elastic-plastic damage constitutive model, which captured the dynamic response of salt caves under seismic loads. In post-earthquake damage assessment studies, Aydan [8] summarized various damage modes of underground structures during earthquakes, while Chen et al. [9] investigated the impact of confining pressure on


H. Bilgin et al. (eds.), *Proceedings of the 2024 6th International Conference on Civil Engineering, Environment Resources and Energy Materials (CCESEM 2024)*, Advances in Engineering Research 253,
https://doi.org/10.2991/978-94-6463-606-2_33

seismic damage. With advancements in numerical computation technologies, numerical simulations have increasingly been applied to the study of seismic damage in caves [10-12]. For instance, Yu et al. [10] utilized a three-dimensional dynamic finite element model to assess the seismic damage effects in tunnels. These studies have significantly advanced the design and stability evaluation of seismic structures.

This paper focuses on the Jiazhaerjia Mountain Cave as a case study. Initially, Prandtl's theory was applied to calculate the design loads. Subsequently, a suitable support scheme was determined through finite element simulation. Finally, the structure was coupled with the surrounding rock to analyze its stability under seismic loads and natural conditions, verifying that the design meets seismic requirements. This study aims to provide analytical insights for the seismic design of similar cave structures.

## 2 Determination of Support Parameters

### 2.1 Engineering Background

The murals on the eastern wall of the Jiazhajia Mountain are a key cultural relic under state protection in China, located 2,088 km from the site of the Shuangjiangkou Hydropower Station on the Dadu River. After the reservoir is filled, the water level will rise 18.4 m above the top of the cave entrance. Consequently, the murals of Jiazhajia Mountain and their surrounding protective areas will be completely submerged, causing devastating damage to the cultural relics. Therefore, it is crucial to protect these valuable artifacts.

To ensure the stability of the cave and avoid damaging the internal murals, an embedded steel arch frame is used to enhance the compressive strength and stability of the cave chamber. Outside the cave, C40 impermeable reinforced concrete is cast, with sidewalls and the roof having a thickness of 1.3 meters and the floor having a thickness of 1.0 meter. The steel arch frame can be well-fitted to the original shape of the cave chamber, minimizing damage to the original site while maintaining a manageable construction difficulty level. The arched structure is designed to primarily withstand axial pressure and thrust (lateral pressure) at both ends to maintain a certain equilibrium. Its load-bearing form is more efficient, and compared to a conventional rectangular structure, it reduces the amount of steel required and optimizes the force distribution.

### 2.2 Pressure of Surrounding Rock

The external loads acting on the arch support are primarily the pressures from the surrounding rock, which include both vertical and horizontal pressures on the steel arch structure. In hard rock strata, the horizontal pressure of the surrounding rock is minimal and can be neglected; however, in soft rock strata, the horizontal pressure is significant and must be considered in calculations.

This paper utilizes Protodyakonov's theory to determine the pressures exerted by the surrounding rock, based on two fundamental assumptions: (1) Considering that the strata are intersected by numerous weak structural planes such as joints and fissures, it is assumed that the surrounding rock can be treated as a loose body to some extent. For

hard rock layers, Protodyakonov suggests compensating for the neglected actual cohesive forces by increasing the inter-particle friction coefficient, referred to as the Protodyakonov coefficient. (2) After the excavation of rock, due to the redistribution of stresses around the cavity, a pressure arch forms above the cavity. The weight of the rock and soil within this arch constitutes the surrounding rock pressure acting on the lining or support structure.

(1) Determination of the Pressure Arch Height

$$\begin{cases} h_1 = \dfrac{a_1}{f} \\ a_1 = a + h\tan(45^\circ - \dfrac{\varphi}{2}) \end{cases} \tag{1}$$

Where, $a$ is half-span of cavern, m; $h$ is Cave height, m; $a_1$ is half-span of pressure arch, m; $\varphi$ is internal friction angle, (°); $f$ is Protodyakonov coefficient.

(2) Determination of the Pressure Arch Stress

After excavation in a loose medium with some cohesive strength, a natural arch forms above it. The vertical pressure acting on the support structure is the weight of the loosened rock mass within the destruction range (natural arch).

Horizontal pressure is considered as a distributed load acting horizontally across the diameter of the cross-section from the arch crown to the bottom of the underground structure, on both sides of the lining. Its magnitude is calculated based on the vertical pressure and the lateral pressure coefficient.

$$\begin{cases} q_1 = \gamma h_1 \\ q_2 = \lambda q_1 \end{cases} \tag{2}$$

Where, $q_1$ is Vertical load, kN/m; $q_2$ Horizontal load, kN/m; $\gamma$ is Permissible weight of surrounding rock, kN/m$^2$; $\lambda$ is lateral pressure coefficient.

The mathematical model is shown in Figure 1.

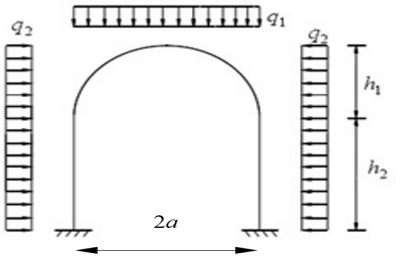


**Fig. 1.** Mathematical model diagram

## 2.3 Design Loads

The loads acting on the structure include: surrounding rock pressure and elastic resistance. In this paper, when calculating the internal forces of the support structure

using a load-structure model, the effect of elastic resistance is temporarily disregarded. The elastic resistance of the strata is beneficial for enhancing the load-bearing capacity of underground structures, but its magnitude and distribution depend on the type of underground structure, its deformation under load, the stiffness of the structure and strata, construction methods, and the deformation properties of the soil layers. Therefore, disregarding the effect of elastic resistance on support is a conservative approach in the design and calculation process. Thus, the loads acting on the structure are horizontal and vertical pressures. The support structure utilizes an integral lining; the arch ring of the integral lining is integrally connected to the sidewalls, and there is generally a rigid connection between the arch foot and the top of the sidewall.

Following Protodyakonov's theory and simplified calculations as discussed previously, the surrounding rock pressure is determined.

$$\begin{cases} q_1 = 27.581 \\ q_2 = 13.791 \end{cases} \tag{3}$$

## 2.4 Steel Arch Design and Calculation

Channel steel C400×100×10.5/18 is selected as the design material for the steel support, arranged in an arch shape according to the different shapes of the caverns. The external loads for each cavern's steel support are determined based on the pressure calculations. Modeling in Abaqus and the application of horizontal and vertical surrounding rock pressures yield displacement and stress diagrams for each section, as shown in Figure 2.

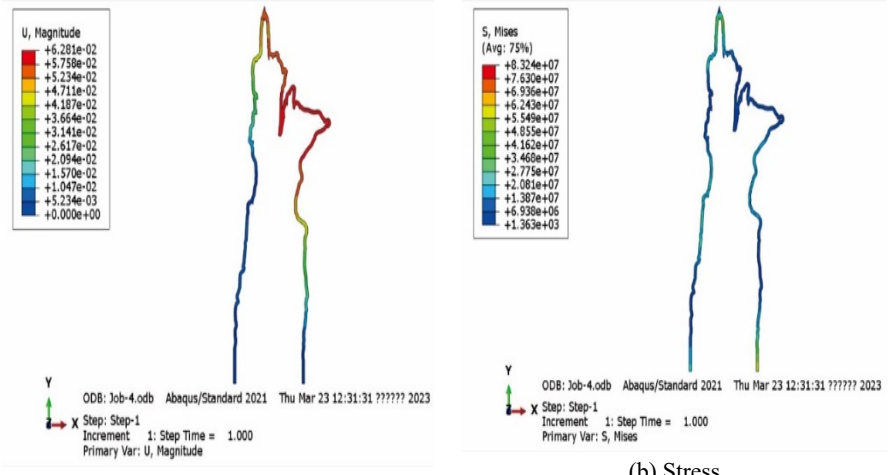


(a) Displacement (b) Stress

**Fig. 2.** Cloud diagram of steel structure simulation

From the diagram, it is observed that the maximum deformation of the steel support after stress application is 8.5 cm, and the minimum is 0 cm. Therefore, the selected structure type satisfies the load-bearing capacity requirements.

## 3 Structural Stability Calculations

Through numerical simulation, the stability of the external structures and the internal artificial stone structures of the cave after relocation and reconstruction is analyzed. Initially, the most hazardous typical section is selected based on the shape of the cave's section after reconstruction as the subject for analysis. The model established, as shown in Figure 3, features a section with a relatively large aspect ratio and artificially shaped stones that are somewhat distorted, making them more prone to stress concentration. This section will utilize ABAQUS software to simulate the stress conditions of each part of the section under natural and seismic conditions, in order to assess their stability.

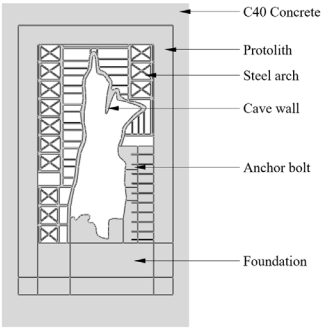


**Fig. 3.** Finite element geometric model

The model comprises five different components, from the exterior to the interior: the existing slope rock and soil body, external concrete wall, steel frame, artificial stone cave wall contour, murals, and internal brick wall. The material parameters for each part are selected as shown in Table 1. Notably, since the steel frame is made of hollow square steel, the material density and modulus of elasticity have been appropriately reduced.

**Table 1.** Mechanical parameters of the model

| Material name | Geotechnical | Concrete | Steel frame | Artificial stone | Brick |
|---|---|---|---|---|---|
| Density/(kg/m$^3$) | 2100 | 2400 | 4000 | 2400 | 2500 |
| Young's modulus /(GPa) | 0.1 | 38 | 100 | 38 | 10 |
| Poisson's ratio | 0.3 | 0.17 | 0.25 | 0.17 | 0.25 |

In the natural condition scenario, the model is subject only to gravity, with the selected gravitational acceleration being g=10 m/s². Under seismic conditions, the structure is subjected to both gravitational and seismic loads. The horizontal direction is typically considered the most hazardous direction for seismic activity. Based on the local seismic intensity level, the peak horizontal acceleration used is ge=0.1g=1 m/s², while the vertical acceleration remains at g=10 m/s². The stress cloud diagrams for natural and seismic conditions are shown in Figure 4, and the displacement cloud diagrams are shown in Figure 5.

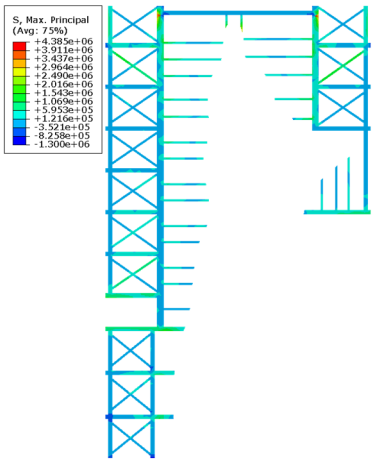


(a) Steel frame - natural condition

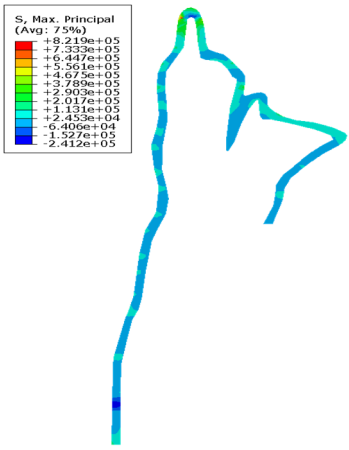


(b) Artificial stone - natural condition

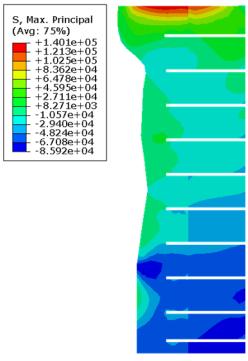


(c) Brick - natural condition

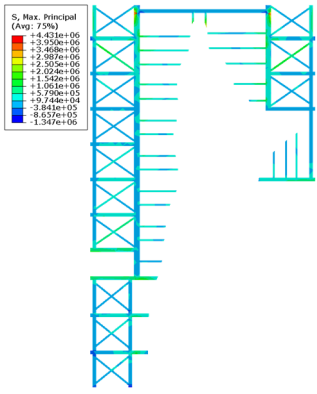


(d) Steel frame - seismic condition

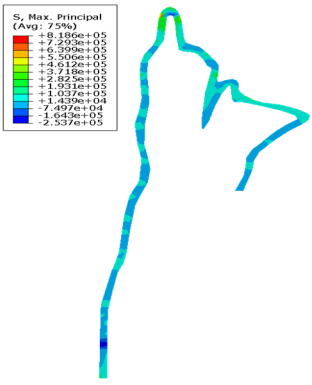


(e) Artificial stone - seismic condition

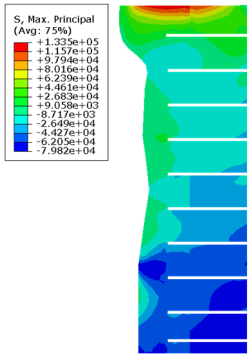


(f) Brick - seismic condition

**Fig. 4.** Stress cloud diagrams

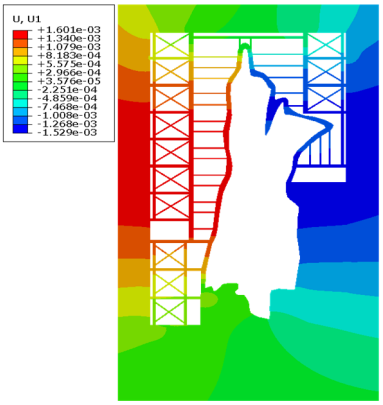


(a) Horizontal displacement- natural condition

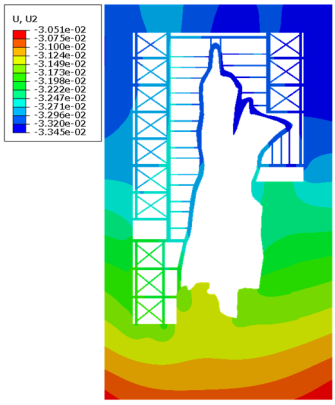


(b) Vertical displacement- natural condition

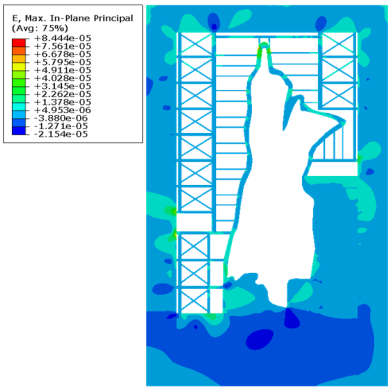


(c) Maximum principal strain- natural condition

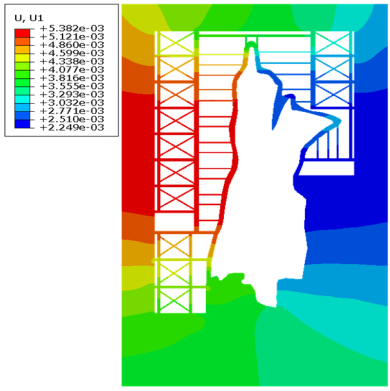


(d) Horizontal displacement- seismic condition

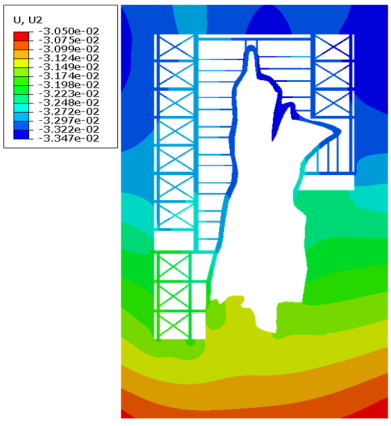


(e) Vertical displacement- seismic condition

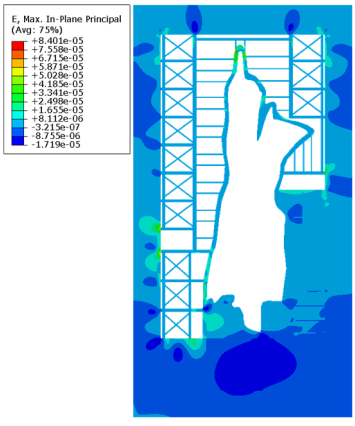


(f) Maximum principal strain- seismic condition

**Fig. 5.** Displacement cloud diagrams

Under natural conditions, the maximum horizontal and vertical displacements are approximately 1.6 mm and 3.05 cm, respectively. Under seismic conditions, the maximum horizontal and vertical displacements are about 5.38 mm and 3.05 cm, respectively; the vertical displacement shows no significant change, while the horizontal displacement along the direction of the earthquake is more pronounced. The overall structure experiences only centimeter-level displacement, manifesting as bulging deformation at the floor level. It is recommended that construction measures take into account the capacity for bulging deformation.

Compared to the natural condition, under the influence of seismic loads, the maximum value of the maximum principal strain actually decreases. In both conditions, the maximum value of the maximum principal strain is only 8.4×10^-5, posing no risk of reaching the yield point.

The maximum principal stress describes the tensile stress condition within the structure, that is, when the maximum principal stress reaches the tensile strength of the material, tensile failure will occur. All results fall within the tensile strength limits of their respective materials, indicating that under the current natural and seismic conditions, the internal and external structures of the cave are within safe limits and there is no risk of failure.

## 4 Conclusion

1. The surrounding rock load was determined using Protodyakonov's theory, and the interface deformation characteristics were analyzed using finite element software to identify the appropriate support scheme.

2. The structural stability under natural conditions and seismic loads was analyzed. The results indicate that the support structure possesses robust seismic performance.

This study has not considered the effects of water permeation. When the water content in the soil increases, the stability of the cave will further decrease. This is an important aspect for future research to consider.

## Acknowledgment

This study was funded by Research projects of C.R.E.C. (2021-key point-34, 2022-key point-01, 2023-major-02).

## Reference

1. Wallis RJ. Art and Shamanism: From Cave Painting to the White Cube. Religions. 2019; 10(1):54. https://doi.org/10.3390/rel10010054.
2. Wu J, Li S C, Xu Z H, et al. Determination of required rock thickness to resist water and mud inrush from karst caves under earthquake action[J]. Tunnelling and Underground Space Technology, 2019, 85: 43-55. https://doi.org/10.1016/j.tust.2018.11.048.

3. Guo Q, Ba J, Luo C. Seismic rock-physics linearized inversion for reservoir-property and pore-type parameters with application to carbonate reservoirs[J]. Geoenergy Science and Engineering, 2023, 224: 211640. https://doi.org/10.1016/j.geoen.2023.211640.
4. Nandi S, Ghosh P. Seismic stability assessment of rock slopes using limiting slope face concept[J]. Rock Mechanics and Rock Engineering, 2023, 56(7): 5077-5102. https://doi.org/10.1007/s00603-023-03308-0.
5. Xu J, Du X. Seismic stability of 3D rock slopes based on a multi-cone failure mechanism[J]. Rock Mechanics and Rock Engineering, 2023, 56(2): 1595-1605. https://doi.org/10.1029/2023GL104080.
6. Lee J, Lumley D E. Interpreting the effects of shale rock properties on seismic anisotropy by statistical and machine learning methods[J]. Geoenergy Science and Engineering, 2023, 224: 211631. https://doi.org/10.1016/j.geoen.2023.211631.
7. Wang T, Yang C, Yan X, et al. Dynamic response of underground gas storage salt cavern under seismic loads[J]. Tunnelling and Underground Space Technology, 2014, 43: 241-252. https://doi.org/10.1016/j.tust.2014.05.020.
8. Aydan Ö, Ohta Y, Geniş M, et al. Response and stability of underground structures in rock mass during earthquakes[J]. Rock mechanics and rock engineering, 2010, 43: 857-875. https://doi.org/10.1007/s00603-010-0105-6.
9. Chen C H, Wang T T, Jeng F S, et al. Mechanisms causing seismic damage of tunnels at different depths[J]. Tunnelling and underground space technology, 2012, 28: 31-40. https://doi.org/10.1016/j.tust.2011.09.001.
10. Yu H, Li Y, Shao X, et al. Virtual hybrid simulation method for underground structures subjected to seismic loadings[J]. Tunnelling and Underground Space Technology, 2021, 110: 103831. https://doi.org/10.1016/j.tust.2021.103831.
11. Dong R, Ping L, Li Y, et al. Seismic deformation mode transformation of rectangular underground structure caused by component failure[J]. Tunnelling and Underground Space Technology, 2020, 98: 103298. https://doi.org/10.1016/j.tust.2020.103298.
12. Li W, Chen Q. Effect of vertical ground motions and overburden depth on the seismic responses of large underground structures[J]. Engineering Structures, 2020, 205: 110073. https://doi.org/10.1016/j.engstruct.2019.110073.